eDSA: Energy-Efficient Dynamic Spectrum Access Protocols for Cognitive Radio Networks

Satyam Agarwal, *Student Member, IEEE*, Swades De, *Senior Member, IEEE*

Abstract—In this paper we propose a class of energy-efficient dynamic spectrum access (DSA) protocols for secondary user (SU) communication over a single primary user (PU) channel. The proposed variants of DSA can be optimized with respect to different back-off strategies and SU packet lengths. Via Markov chain models and numerical analysis, we derive the optimal SU packet length and inter-sensing time for optimal SU performance in the DSA variants. We evaluate the protocol performance in terms of SU goodput, SU energy efficiency, and PU collision ratio. Adaptability of the proposed SU operation protocol in practical scenarios is tested over cellular GSM band as well as under real-time video over IP based PU traffic in ISM band. Our performance studies demonstrate that the proposed protocols offer significantly high channel utilization while keeping the PU collisions below an acceptable threshold. The proposed protocol operation is also outlined, where the protocol adapts to the changing PU traffic load for optimized performance.

Index Terms—Dynamic spectrum access, cognitive radio access protocols, secondary user goodput, energy efficiency, Markov chain

1 Introduction

The spectrum access in cognitive radio (CR) networks (CRNs) can be classified into two: 'white space access' (WSA) [1], and 'dynamic spectrum access' (DSA) [2]. In WSA, the spectrum availability is reasonably static and predetermined. As a result, the WSA strategy by the CRs is typically based on spectrum usage database. The secondary users (SUs) in such cases simply access the database to decide on the spectrum usage coordination at the time of their needs; they may not have any spectrum sensing capability. Typical example of WSA is the use of TV 'white space' [3]. In DSA, on the other hand, the spectrum availability is much more dynamic, spatially as well as temporally. Therefore, it may be more prudent to have the SUs that are capable of sensing the channel availability locally and exploiting the spatio-temporal voids. The typical applications of DSA with the SUs spectrum sensing capability are secondary usage in the conventional licensed cellular operation bands [4]. *In this study, we focus on dynamic spectrum access by SUs over an agile primary user (PU) channel with SUs having spectrum sensing capability.*

In DSA, the two key aspects of interest are: maximized utilization of unused PU channel and energy-efficient operation of the SUs [5]. While reduced SU packet size may increase the utilization with limited interference to the PUs [6], due to finite-sized packet header optimal SU packet size would maximize the SU data transmission efficiency. On the other hand, for maximized energy efficiency, the SUs should sense the PU channel only at optimally-chosen intervals.

1.1 Key objectives

This paper aims at the following key issues: (a) designing energy-efficient spectrum access policy in an agile PU channel; (b) ensuring high utilization of channel while meeting the PU interference constraint; (c) joint optimization of SU packet lengths and inter-sensing intervals; (d) providing guidelines for practically implementable protocol on a low-cost SU platform.

The different performance metrics are defined as follows:

Definition 1. *SU goodput is the amount of data payload that can be transmitted over the channel per unit time.*

Definition 2. *SU energy efficiency is the amount of data payload transmitted by SU per unit energy consumption.*

Definition 3. *PU collision ratio is the proportion of time SUs' transmission interferes (overlaps) with the PU transmission.*

We propose three novel protocol variants for energy-efficient DSA, namely, eDSA V.1, eDSA V.2, and eDSA V.3. The protocols jointly account for optimal inter-sensing time and SU packet lengths, which is expected to increase the SU throughput while keeping overheads and hence the energy consumption low. We analyze the SU goodput, SU energy efficiency, and PU collision ratio. In design and analysis of the protocol performance, practical aspects for packet transmission are considered, where the packets are sent along with some overhead and block coding schemes.

Two optimization problems are formulated for maximizing respectively the SU goodput and SU energy efficiency, with a bound on the PU collision ratio. For a given PU channel condition, we obtain the optimal SU packet size and optimal channel inter-sensing time, such that the above performances are maximized. Since the optimal performance depends on the PU channel parameters, we suggest a heuristic for the SU to estimate the traffic. A SU maintains a look-up table, complemented with pattern search algorithm, to provide quickly adaptive optimal operating parameters in dynamic traffic conditions. Experiments are carried out over real PU traffic traces to demonstrate the operation of the proposed protocols. The results show that the protocols perform significantly better than the competitive ones in [7] and [8].

1.2 Contributions

The main contributions of the paper are as follows: (i) The proposed eDSA protocol variants offer adjustability of the SU

S. Agarwal and S. De are with the Department of Electrical Engineering and Bharti School of Telecom, Indian Institute of Technology Delhi, India.
Email: {satyam.agarwal,swadesd}@ee.iitd.ac.in

activity, leading to significantly improved spectrum usage performance. The protocols can be optimized for SU goodput as well as energy efficiency maximization. (ii) The theoretical optimization formulations provide a solid mathematical basis on the improved performance of the proposed protocols. (iii) The protocol operation over GSM bands as well as under real-time video over IP traffic based PU activity in ISM band are carried out to show their practical utility. (iv) The suggested look-up table, along with low-complexity augmented Lagrange pattern search algorithm, for optimal SU parameters in dynamic PU activity environments aids to simplicity and practicality of the protocols.

The proposed protocol variants in this paper can be of interest in many applications. For example, in CR sensor networks (CRSNs), where the field sensors need to send the field data to a remote sink, lifetime of the field node is of prime concern. Therefore, the sensors may do well by not sensing the channel bands frequently to aid channel switching [9]. Instead, by remaining static in a chosen/given band, it will be energy-efficient if the channel is sensed at some judiciously chosen intervals. Clearly, if the spectrum allocation to the sensor nodes can be static, it further reduces the hardware and network operation cost. The study here is also applicable to WLAN, cellular, and other agile PU traffic scenarios, where the SUs may exploit opportunities between the packet bursts.

1.3 Scope of paper

The access schemes proposed in this paper apply to a pair of SUs operating on a single PU channel. The channel is accessed by only a pair of SU at a time, hence, no multiuser contention is required. The SU while operating on a PU channel aims to make full use of the available spaces in the channel. Although cooperative spectrum sensing [10], [11] provides high sensing reliability, since this paper deals with the spectrum access issues for operation of a single SU pair over a PU channel, in this paper we consider single SU alone for channel sensing. The effects of imperfect channel sensing and channel fading are accounted in this paper by considering coded transmission framework.

1.4 Paper organization

The next section surveys the related works. In Section 3 the proposed system model and protocol operations are described. Section 4 deals with the protocol performance analysis using Markov chain models. Section 5 discusses the practical implementation aspects of the protocols. Section 6 presents the numerical results. The paper is concluded in Section 7.

2 Related Works

Various CR spectrum access protocols have been proposed in the literature. A detailed survey can be found in [12]. In [13], multiple channels are allocated to a pair of SUs, and a SU finds the optimal sequence of channel sensing and optimal sensing period to maximize the access opportunities with minimum channel switching latency. In [7], the authors proposed three access schemes for the SU operation and investigated the SU throughput. They defined two different types of collision with PU: in one, the entire PU packet is lost in case of SU transmission collision, while in the other, only a portion of PU transmission overlapping with SUs transmission is lost. Lower and upper bounds on the maximum throughput achievable by the SU was derived in [6]. They also proposed an optimal spectrum access policy for the cases of perfect as well as imperfect spectrum sensing. The effects of SU packet length, overheads, and sensing time were not accounted.

A scheme to exploit the opportunities in between packet bursts was presented in [14]. Time was divided into frames, which was further subdivided into channel learning subframe and channel access subframe. In channel learning subframe, SU learns the PU occupancy characteristics by employing a hidden Markov model (HMM). In contrast, in channel access subframe, SU predicts the channel state using partially observable Markov decision process (POMDP) and decides on whether to access the channel or to switch to another channel. [15] took the case of non-agile SU (where the SU does not have channel switching capability). In their proposed access policy decision is taken in each slot according to the state in the previous slot, where the slots are categorized into one of the four states, namely, channel idle, channel busy, SU transmission successful, and SU transmission failed.

A transmission probability scheduling (TPS) scheme was proposed in [16], where the SUs maximize their throughput by optimally scheduling their transmission probabilities in each idle slot based on the PU traffic pattern. [17] presented the operation of multiple SUs over a single PU channel. Normal spectrum sensing is performed at the beginning of each frame, while fast spectrum sensing is performed after successful contention to check for the random arrival of PU. Authors in [18] proposed a CR based carrier sense medium access with collision avoidance (CR-CSMA/CA) which is based on the asynchronous spectrum sensing and request to send/clear to send (RTS/CTS) handshake. The SUs having packet to transmit first sense the channel and start the negotiation phase with the transmission of RTS. Successful contention is followed by transmission of data packet over the channel. Multiple SUs contending for the channel at the same time reduces the throughput of the CRNs. In [19], [20], common control channel was employed by the SUs to contend for the available channels. On successful contention, the SUs occupy the reserved PU channel and start transmission.

The above mentioned access schemes do not account for the energy consumption, which is critical for battery operated SUs. In [21], sensing energy is minimized by optimally adjusting the spectrum sensing period while constraining the undiscovered spectrum opportunities. In [22], optimum sensing time and sensing duty cycle were computed to make the spectrum sensors energy efficient. In [23], [24], optimum sensing duration and transmission times were jointly determined for energy efficiency. [25] considered PUs operation on a time slotted channel and optimized the SU transmission rate in each slot based on the delay in data transmission and SU energy consumption in channel sensing and idling. Energy efficient packet size optimization in CRSN was studied in [26], where the results showed that the optimal packet size depends significantly on the channel BER and PU behavior in the channel. However, these approaches do not address the channel inter-sensing time and SU packet lengths jointly.

The authors in [27] considered a single SU accessing multiple PU channels in an energy efficient manner. Channel switching energy consumption was incorporated into the optimization problem and simulation results were provided to show the protocol performance. [28] proposed an energy-efficient opportunistic spectrum access in orthogonal frequency division multiplexing (OFDM) based CRN. Optimization of unused subchannel assignment to different SUs and transmission power of SU over the PU channels is done within PU interference constraints. A cognitive adaptive

MAC (CAMAC) for CRSNs was presented in [29], where the SUs conserve energy on three fronts: on-demand spectrum sensing, limiting the number of spectrum sensing nodes, and periodic sleeping of the CR nodes and waking up whenever the data is present for transmission. In a residual idle time distribution based scheme (RIBS) for channel access [8], the channel is sensed at random instances and the SU estimates the transmission duration based on the RIBS. This scheme is claimed to be energy efficient because periodic sensing is not required, however the channel utilization is expected to be low due to random channel sensing.

In view of the existing literature, *we argue that one important aspect that needs to be considered is the joint optimization of channel inter-sensing times and SU packet lengths, which is critical for high idle channel utilization and energy-efficient performance of the SUs*. To this end, *the proposed protocol variants in the current work is a new direction to maximize the SUs energy efficiency in a dynamic PU environment*.

With respect to system settings, our approach is close to the schemes in [7], [8], though it has a few contrasting features. First, the existing works (e.g., [7], [8]) typically assume that the SU packet lengths are very small compared to the length of PU packets. However, in practice, SU and PU packet lengths can be comparable, and the collision of a SU packet can span over more than one PU packet. Second, in the existing protocols the PU collision ratio is defined as the number of PU packets interfered. However, in scenarios where the PU traffic is comprised of voice or video or a large chunk of data, they are always transmitted with forward error control (FEC) coding, and if a small portion of a packet is garbled, the packet may still be recoverable at the receiver with the help of FEC.

3 System Model and Protocol Description

3.1 System model

We consider a scenario where a pair of CR-enabled SUs are seeking to access a PU channel for their communication. There may be many PUs operating on the same band. PUs operate on non-CSMA protocol. The proposed eDSA protocols can be applicable in any PU activity scenario (time-slotted or unslotted), without requiring any synchronization with the PU network. SUs are looking for temporal availability in this PU channel. For studying the maximum possible secondary usage, we consider a SU always has data for transmission with the capability of forming packets of any size. The SU pair is considered to experience the same PU channel availability condition. When the SU communication range is small compared to the PU base station coverage, this is a reasonable assumption on [6], [15].

SU senses the channel for detection of PU activity. The outcome could be either 'busy' or 'idle'. The operation of PU is characterized as an ON-OFF model with 'busy' and 'idle' periods distributed exponentially, with respective averages μ and λ. The channel is temporally divided into slots of equal size of duration T seconds. Without loss of generality, we consider 1-slot sensing (T can be variable). The time slots are small with respect to the scale of λ and μ. So the PU activity state can be considered quasi-static within a slot interval.

The quality of channel sensing depends on the amount of time the SU senses the channel. We consider the case of imperfect sensing, where the SU misdetects a busy channel with probability p_{md} and raises false alarm against the idle channel with probability p_{fa}. Additionally, the wireless channel between the SU transmitter and receiver is considered slow Rayleigh fading channel. Following [30], two state Gilbert-Elliot model is used to characterize the burst error process in the channel. The channel occupies one of the two states, Good and Bad. In Good state, the signal-to-noise ratio (SNR) at SU is acceptable to receive the transmission with a small probability of error, while in Bad state the channel is dominated by noise and hence the packet is lost.

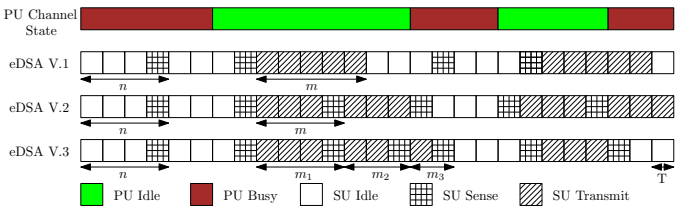

Fig. 1: Different operation phases of the proposed eDSA protocols.

3.2 Protocol description

With the slotted system time, channel is sensed in some slots, while data transmission is carried out in other slots if the channel is detected idle. SUs perform half-duplex communication. There are two phases of operation, namely, spectrum sensing phase and data transmission phase.

In *spectrum sensing phase*, if the channel is sensed busy, the SU remains in this phase and enters into idle mode for a specified duration. The cycle of sensing and idling is repeated until the channel is sensed to be idle, when the SU enters the data transmission phase. In *data transmission phase*, the SU transmits data for some chosen amount of time.

We propose three versions of the eDSA protocol.

eDSA V.1: The spectrum sensing phase consists of n slots. For the first $n-1$ slots the SU remains idle, while in the last slot the channel is sensed. The optimal value of n is determined such that in these n slots the PUs activity is expected to be over. As long as the channel is sensed busy, this sensing phase continues. If the channel is sensed idle, the SU moves to the data transmission phase. SU in the data transmission phase transmits for m consecutive slots. The SU forms a packet of size (duration) m slots and transmits it. A PU may arrive in between a SU packet transmission, resulting in a collision. For the SU we assume that the data is encapsulated with FEC bits. So, if the collision is within the allowable error range of the packet, it is successfully received. After transmission of a packet, the SU goes back to spectrum sensing phase.

eDSA V.2: In eDSA V.1, for every packet transmission the SU has to sense the channel – which could be wasteful from channel utilization viewpoint. For an improved channel utilization, we propose a modification – called eDSA V.2. Here, the data transmission phase consists of m slots. A packet of length $m-1$ slot duration is transmitted, while the last slot is utilized for sensing the channel for PU activity. If the channel is found to be idle, another SU packet is transmitted in the next $m-1$ slots, and the process is repeated. If instead the channel is found busy, the SU returns to the spectrum sensing phase with n slots periodicity, as in eDSA V.1.

eDSA V.3: In eDSA V.2, all successive data packets are of equal length. However, since the ON-OFF behavior (combined ON and OFF duration) of PU activity is not memoryless, it could be beneficial to account for the history of successive SU packet

transmissions in deciding the next packet size. Therefore, in eDSA V.3, to achieve high SU goodput, we propose to vary the SU packet size in successive transmissions. In kth order eDSA V.3, up to k-phases of successive data packets, the size (in slots) is varied as $m_1 - 1,\ m_2 - 1,\ \cdots, m_k - 1$. Phase i to $i+1$ is progressed if in the last slot of phase i the PU channel is sensed idle. Beyond the kth phase, if the channel is still found idle (in the last slot of the previous phase), the transmitted data packet size is kept at $m_k - 1$. This process continues until the channel is found busy – triggering a fresh sensing phase of n slot periodicity. In this paper, we consider $k = 3$. So, the adjustable parameters in eDSA V.3 performance optimization are m_1, m_2, m_3, and n.

Fig. 1 shows the different phases of the eDSA protocols, with $n = 4$ slots, $m = 5$ for eDSA V.1, $m = 4$ for eDSA V.2, and $m_1 = 4$, $m_2 = 3$, and $m_3 = 2$ for eDSA V.3.

TABLE 1: List of variables and their descriptions.

C_k	Channel state in slot k
λ	Average PU 'OFF' period
μ	Average PU 'ON' period
R_c	PU collision ratio
$\mathcal{G}$	Goodput of SU
$\mathcal{E}$	Energy efficiency of SU
$\mathbf{P}$	System state transition probability matrix
k_e	Ratio of maximum allowable error to total packet size
k_c	Ratio of input and output bits in error coding block
b	Number of bits transmitted per slot
d_k	Number of bits transmitted in k slots, $b \cdot k$
Φ_t	Energy consumption in transmission per slot
Φ_s	Energy consumption in sensing per slot
Φ_i	Idle energy consumption per slot
H	Overhead per packet
F	Fading margin (dB)
f_D	Doppler frequency
v_c	SU velocity (m/s)
p_{fa}	Probability of false alarm
p_{md}	Probability of misdetection

4 Performance Analysis

In this section, we first analytically characterize the performance of the proposed protocol variants in terms of SU goodput, SU energy efficiency, and PU collision ratio. Then, via optimization formulations, the optimum sensing interval and data transmission duration are obtained. Table 1 shows the list of variables used, along with the descriptions.

4.1 Performance measures

SU Goodput: Let the SU packet size (including overhead) be d bits and k_c denote the fraction of bits representing payload in the encoded message bits. Let H be the header length. By Definition 1 in Section 1.1, we have:

$$\mathcal{G} = \lim_{t\to\infty} \frac{\begin{array}{c}(d \cdot k_c - H) \cdot \Pr\{\text{Receive success}\} \\ \times \text{ Number of packets transmitted in time } t\end{array}}{\text{Total time } t}. \quad (1)$$

SU energy efficiency: By Definition 2 in Section 1.1, the goodput achievable per unit energy is:

$$\mathcal{E} = \frac{\text{SU Goodput}}{\text{Power consumption by SU}}. \quad (2)$$

PU collision ratio: Recalling that the SU packet size could be comparable to that of the PU's and the PU packet transmissions may be interfered at more than one busy periods, as per Definition 3 in Section 1.1, in a slotted communication PU collision ratio can be expressed as:

$$\mathcal{R}_c = \frac{\text{Number of slots in which PU experienced collision}}{\text{Number of slots in which PU transmitted}}. \quad (3)$$

4.2 Channel availability characterization

In the ON-OFF channel model, the PU channel state at any slot can be represented in terms of Markov model with the states ON and OFF. Each slot is of duration T seconds.

Define a random variable C_k, Denoting the channel state in slot k by a random variable C_k,

$$C_k = \begin{cases} 1 & \text{if channel is busy (ON) in slot } k \\ 0 & \text{if channel is idle (OFF) in slot } k. \end{cases}$$

Since the ON and OFF periods are exponentially distributed, the PU channel state transition probability from OFF to ON state can be obtained as:

$$Pr[OFF \to ON] \triangleq p_{01} = \int_0^T \frac{1}{\lambda} e^{-x/\lambda}\, dx = 1 - e^{-T/\lambda}.$$

Similarly, the other transition probabilities can be obtained. The resultant one-step transition probability matrix of the Markov chain represented by states ON and OFF is given as:

$$\mathbf{P}_c = \begin{bmatrix} e^{-T/\lambda} & 1 - e^{-T/\lambda} \\ 1 - e^{-T/\mu} & e^{-T/\mu} \end{bmatrix}. \quad (4)$$

The SU transmission is performed over a slow Rayleigh fading channel. The Markov chain for the SU channel model consists of two states, namely, Good (g) and Bad (b). The transition probabilities between the two states in terms of fading margin F and Doppler frequency f_D are given as [30]:

$$\delta = 1 - e^{-1/F},\ p_{bg} \triangleq Pr(b,g) = \frac{Q(\theta, \sigma\theta) - Q(\sigma\theta, \theta)}{e^{1/F} - 1}$$

$$p_{gg} \triangleq Pr(g,g) = 1 - \frac{p_{bg}\delta}{1-\delta}.$$

Here $\theta = \sqrt{2/F(1-\sigma^2)}$, $Q(\cdot,\cdot)$ is the Marcum Q function, $\sigma = J_0(2\pi f_D T)$ is the correlation coefficient, and $J_0(\cdot)$ is the Bessel function of first kind and zeroth order. $\mathbf{P}_F$ denotes the one-step transition probability matrix of the SU channel states and is given as:

$$\mathbf{P}_F = \begin{bmatrix} p_{gg} & 1 - p_{gg} \\ p_{bg} & 1 - p_{bg} \end{bmatrix}. \quad (5)$$

The system state is a combination of PU channel state representing PU activity and SU channel state accounting fading state of the channel between SU transmitter and receiver. The resultant Markov chain representation of the system state transition is shown in Fig. 2. $\mathcal{S} = \{A,\ B,\ C,\ D\}$ denotes the set of states in the system Markov chain. The transition probability from state A to state D is $p_{01}p_{gb}$. Similarly, the other transition probabilities are computed in the one-step state transition probability matrix $\mathbf{P} = \mathbf{P}_c \bigotimes \mathbf{P}_F$, where $\bigotimes$ is Kronecker product of two matrices.

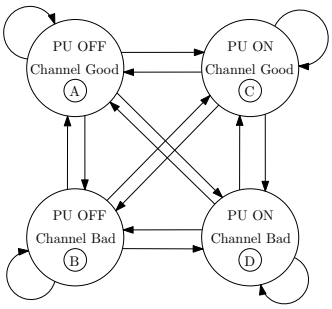

Fig. 2: Representation of channel availability states.

In energy detector based sensing with sampling frequency f_s, channel sensing time T, and sensing threshold ϵ, the false alarm and misdetection probabilities are given as [31]:

$$p_{md}(\epsilon, T) = \text{erfc}\left(\left(\frac{\epsilon}{\sigma_u^2} - \gamma - 1\right)\sqrt{\frac{Tf_s}{2\gamma+1}}\right) \quad (6)$$

$$p_{fa}(\epsilon, T) = \text{erfc}\left(\left(\frac{\epsilon}{\sigma_u^2} - 1\right)\sqrt{Tf_s}\right) \quad (7)$$

where γ is the received SNR at the SU due to PU transmission and σ_u^2 is the noise power variance.

4.3 SU activity dependent system performance

Based on the channel availability information in Section 4.2, we evaluate the effects on data transmission of SU and PU.

4.3.1 Success probability of SU packet transmission

A SU transmits packets whenever it senses the channel is idle. A FEC coded SU packet of size l slots is successful if $1 - k_e$ fraction is correctly decoded at the receiver, where k_e is the ratio of maximum allowable error in a packet (bits) to the data packet size (bits). A data packet loss is partly due to overlapping PU activity and partly due to SU channel fading. We define a Markov chain to represent the SU packet transmission of length l slots over the channel (Fig. 3).

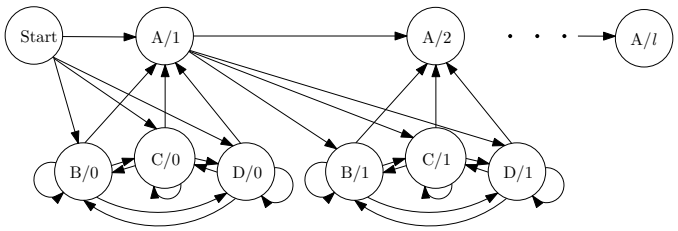

Fig. 3: Markov chain representation of l slot SU packet transmission.

At some slot k, the states in the Markov chain is defined by two variables: the system state in slot k, and the number of successful slots up to slot k. The system states are one of the four states $\mathcal{S} = \{A, B, C, D\}$ (cf. Fig. 2). The SU can enter the data transmission phase at any of the four states. This state is denoted as the 'start' state in Fig. 3. If the transition happens to state A, the receiver can decode the transmission successfully in the first slot, hence next state is A/1. If instead the next system state is B, C, or D, SU transmission in this slot is lost, hence the next state would be B/0, C/0, or D/0. Likewise, the other transitions are carried out.

In a homogeneous PU activity scenario, the one-step state transition probabilities of the Markov chain can be obtained using $\mathbf{P}$. For example, the one-step transition probability from state A/1 to A/2 is $\mathbf{P}(A, A)$, and transition from state A/1 to D/1 is $\mathbf{P}(A, D)$. Similarly the other transition probabilities of the Markov chain can be computed. For a packet transmission of length l slots, we need to consider the Markov chain up to state A/l. Denote the one-step transition probability matrix of the Markov chain as $\mathbf{Q}_s$ with start state $s \in \mathcal{S}$. $\mathbf{Q}_s^l$ is the l-step transition probability of the Markov chain. The probability of successful packet transmission by a SU in l slots starting with system state $s \in \mathcal{S}$ ('start' $= s$) with the error tolerance k_e is given as:

$$p_s(l, s) = \mathbf{Q}_s^l(s, A/l) + \sum_{z \in \mathcal{S}} \sum_{i=\lfloor l \cdot (1-k_e) \rfloor}^{l-1} \mathbf{Q}_s^l(s, z/i). \quad (8)$$

4.3.2 PU activity dependent channel state transitions

PU transmissions can happen during SU's channel sensing or data transmission phase. The expected number of slots PU occupies in each phase of SU operation is of interest. Channel state transition due to PU activity is shown in Fig. 4.

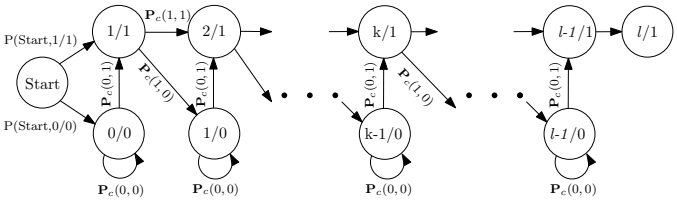

Fig. 4: PU activity dependent channel state transitions.

The channel state in some slot k is defined by two variables: the number of slots PU transmitted up to slot k (excluding 'start' state), and the PU activity ('0' (OFF)/'1' (ON)) in slot k. The 'start' state is the PU activity state from which the SU enters a particular phase. If the SU enters a particular phase when PU channel is busy, the start state is denoted by 0/1. In the next slot, if the channel is busy, the system transits to state 1/1, else the next state is 0/0. The transition probabilities are defined utilizing $\mathbf{P_c}$ in (4). One-step transition probability from state 1/1 to 1/0 is $\mathbf{P_c}(1, 0)$. Similarly other transition probabilities can be specified. In a phase of length l slots, the states in the Markov chain can be up to $l/1$. We denote one-step transition probability matrix as $\mathbf{U}_s$. With 'start' state $s \in \mathcal{S}$, where states A and B correspond to PU channel state 0 (OFF) and states C and D correspond to PU channel state 1 (ON) (cf. Fig. 2), $\mathbf{U}_s^l$ is the l-step transition probability matrix. With the probability distribution of number of slots occupied by PU in an l-slot phase starting with state s, the expected number of slots with PU collision can be calculated as:

$$E_p(l, s) = \sum_{i=1}^{l} i \cdot \{\mathbf{U}_s^l(s, 0/i) + \mathbf{U}_s^l(s, 1/i)\}. \quad (9)$$

With the knowledge of SU packet transmission success probability and PU collision in the SU data transmission phase, we characterize the eDSA protocol dependent SU states.

4.4 Characterization of SU states

We characterize the proposed eDSA protocol versions via finite state machine (FSM) representation of the SU states.

eDSA V.1: In this version there are eight SU system states in the FSM: four corresponding to the spectrum sensing phase of n

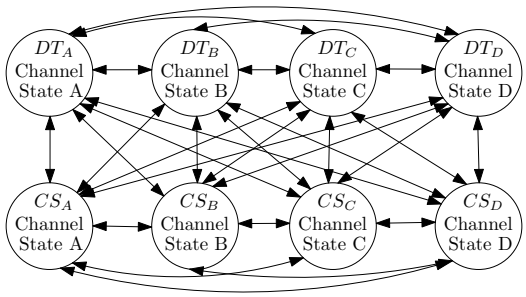

Fig. 5: FSM representation of eDSA V.1 and eDSA V.2.

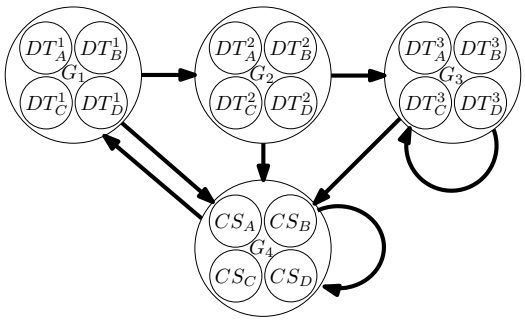

Fig. 6: FSM representation of eDSA V.3.

slots duration each (denoted as CS), and four for the combination of a data transmission phase of m slots followed by spectrum sensing phase of n slots (denoted as DT), as shown in Fig. 5. Thus, in eDSA V.1, the DT states are of duration $m+n$ slots, whereas the CS states are of duration n slots. Each of the DT and CS states correspond to the four channel states (cf. Fig. 2) from which the SU can enter a particular phase. For example, if the SU encounters *good* and *idle* (OFF) PU channel in the sensing slot and chooses to enter data transmission phase, the system state is DT_A. Similarly, if the SU encounters *bad* (deep fading) and *idle* PU channel and chooses to enter spectrum sensing phase, the system transits to state CS_B. The choice made by the SU depends on the channel sensing observation, influenced by sensing imperfections (false alarm and misdetection).

One-step transition probabilities of these states could be obtained using $\mathbf{P}$, p_{fa}, and p_{md}. For example, transition from state DT_A to CS_C involves the transition of channel state from A to C in $m+n$ slots and the channel is correctly detected busy by SU. Hence the one-step transition probability for this case is $\mathbf{P}^{m+n}(A,C)(1-p_{md})$. Similarly, the other transitions for this Markov chain could be specified. We denote the overall state transition probability matrix in eDSA V.1 by $\mathbf{W}_{V_1}$.

eDSA V.2: This version as well is represented by an eight state Markov chain, shown in Fig. 5. Here the DT states correspond to the data transmission phase of m slots, where a packet of $m-1$ slots is transmitted followed by channel sensing in the last slot. A CS state corresponds to the spectrum sensing phase of n slots, where the SU remains idle for $n-1$ slots and the channel is sensed in the last slot. One-step transition probabilities are defined similarly as in eDSA V.1. We denote the overall state transition probability matrix in eDSA V.2 by $\mathbf{W}_{V_2}$.

eDSA V.3: In this version there are 16 states grouped into four, as shown in Fig. 6. The three groups G_1, G_2, and G_3 correspond to the data transmission phases of length m_1, m_2, and m_3 slots, respectively, while the last group G_4 corresponds to the spectrum sensing phase of length n slots. Each of the groups contain 4 states corresponding to the channel states in $\mathcal{S}$. The transition from states of G_1 to states of G_2 occurs when the SU decides to continue transmission after the transmission of packet of length m_1-1 slots. Similarly, the transition from G_2 to G_3 occurs when the SU chooses to transmit another packet of length m_3-1 after the transmission of packet of length m_2-1 slots. The SU transits to the spectrum sensing phase G_4, if it senses the channel to be busy at the end of a data transmission phase. The one-step transition probability can be obtained similarly as in eDSA V.1. We denote the overall state transition probability matrix in eDSA V.3 as $\mathbf{W}_{V_3}$.

With the knowledge of state transition probabilities of a protocol version, the limiting probabilities $\underline{\pi}$ of these states are determined using the matrix equation:

$$\underline{\pi}^{V_i} = \underline{\pi}^{V_i} \cdot \mathbf{W}_{V_i}$$

where $\underline{\pi}^{V_i}$ is the limiting probability vector of protocol version $i=1,2,3$. Recall that, $\sum_{k\in\text{all states}} \pi^{V_i}(k) = 1$.

We now quantify the SU performance and PU collisions.

4.5 SU goodput

Following the definition in (1) and using (8), goodput of the different versions of the protocol are obtained as:

eDSA V.1:

$$\mathcal{G}^{V_1}(\mathbf{m},n) = \frac{\sum_{s\in\mathcal{S}} \pi^{V_1}(DT_s)\cdot(d_m\cdot k_c - H)\cdot p_s(m,s)}{T\sum_{s\in\mathcal{S}}\{(m+n)\pi^{V_1}(DT_s) + n\pi^{V_1}(CS_s)\}} \quad (9)$$

where d_m is the number of data bits transmitted in m slots (Table 1).

eDSA V.2:

$$\mathcal{G}^{V_2}(\mathbf{m},n) = \frac{\sum_{s\in\mathcal{S}} \pi^{V_2}(DT_s)\cdot(d_{m-1}\cdot k_c - H)\cdot p_s(m-1,s)}{T\sum_{s\in\mathcal{S}}\{m\pi^{V_2}(DT_s) + n\pi^{V_2}(CS_s)\}}. \quad (10)$$

eDSA V.3:

$$\mathcal{G}^{V_3}(\mathbf{m},n) = \frac{\sum_{j=1}^{3}\sum_{s\in\mathcal{S}} \pi^{V_3}(DT_s^j)\cdot(d_{m_j-1}\cdot k_c - H)\cdot p_s(m_j-1,s)}{T\sum_{s\in\mathcal{S}}\{\sum_{j=1}^{3}\{m_j\pi^{V_3}(DT_s^j) + n\pi^{V_3}(CS_s)\}\}}. \quad (11)$$

For eDSA V.1 and eDSA V.2, $\mathbf{m} = m$; for eDSA V.3 with three steps of transmitted packet size, $\mathbf{m} = (m_1, m_2, m_3)$.

4.6 SU energy efficiency

We denote the energy consumption per slot as: Φ_s for channel sensing, Φ_t for data transmission, and Φ_i in the SU idling state.

eDSA V.1: The energy consumption in a DT state is $m\Phi_t + (n-1)\Phi_i + \Phi_s$ (m slots data, $(n-1)$ slots idle, and 1 slot sensing) while in CS states it is $\Phi_s + \Phi_i\cdot(n-1)$. The average power consumption is given by (12).

eDSA V.2: In eDSA V.2, recall that, in packet transmission phase, the data is transmitted over $m-1$ slots while the last slot is for sensing. So, the energy consumption in a DT state is $\Phi_t\cdot(m-1) + \Phi_s$ and in a CS state is $\Phi_s + \Phi_i\cdot(n-1)$. The average power consumption is given in (13).

eDSA V.3: In this case, for states in group G_1, G_2, and G_3, data is transmitted over m_1-1, m_2-1, and m_3-1 slots, respectively; the last slot is for sensing. So, the energy consumption

for states in groups G_1, G_2, and G_3, are $\Phi_t \cdot (m_1 - 1) + \Phi_s$, $\Phi_t \cdot (m_2 - 1) + \Phi_s$, and $\Phi_t \cdot (m_3 - 1) + \Phi_s$ respectively, while for states in group G_4 it is $\Phi_s + \Phi_i \cdot (n - 1)$. Accordingly, the average power consumption is given by (14).

The SU energy efficiency can be computed as

$$\mathcal{E}^{V_i} = \frac{\mathcal{G}^{V_i}}{\Phi^{V_i}}. \tag{15}$$

4.7 PU collision ratio

PU collision ratio captures the PU performance degradation in presence of SU activities. Following the Definition 3, this can be obtained in the different SU protocol versions as follows:

eDSA V.1:

$$R_c^{V_1}(\mathbf{m}, n) = \frac{\sum_{s\in\mathcal{S}} \pi^{V_1}(DT_s) \cdot E_p(m, s)}{\sum_{s\in\mathcal{S}}\{\pi^{V_1}(DT_s) \cdot E_p(m+n, s) + \pi^{V_1}(CS_s) \cdot E_p(n, s)\}} \tag{16}$$

eDSA V.2:

$$R_c^{V_2}(\mathbf{m}, n) = \frac{\sum_{s\in\mathcal{S}} \pi^{V_2}(DT_s) \cdot E_p(m-1, s)}{\sum_{s\in\mathcal{S}}\{\pi^{V_2}(DT_s) \cdot E_p(m, s) + \pi^{V_2}(CS_s) \cdot E_p(n, s)\}} \tag{17}$$

eDSA V.3:

$$R_c^{V_3}(\mathbf{m}, n) = \frac{\sum_{s\in\mathcal{S}} \sum_{j=1}^{3} \pi^{V_3}(DT_s^j) E_p(m_j - 1, s)}{\sum_{s\in\mathcal{S}}\{\sum_{j=1}^{3}\{\pi^{V_3}(DT_s^j) E_p(m_j, s) + \pi^{V_3}(CS_s) E_p(n, s)\}\}}. \tag{18}$$

4.8 Protocol parameters optimization

A natural question arises on the suitable choice of data packet lengths and sensing phase duration, so that the optimum SU performance can be achieved at a bounded cost of PU performance degradation. In other words, data transmission phase and spectrum sensing phase lengths need to be optimized to maximize the SU performance. We define two constrained optimization problems for the proposed protocol variants. The first optimization problem that maximizes the SU goodput in a given PU traffic condition while ensuring that the interference caused to PU remains below a certain chosen threshold, is formulated as:

$$\begin{aligned} (P1)\ \ & \mathcal{G}_{opt}^{V_i} = \max_{\mathbf{m},n} \left\{\mathcal{G}^{V_i}(\mathbf{m}, n)\right\} \\ \text{s.t. } & R_c^{V_i}(\mathbf{m}, n) \le \eta \\ & \mathbf{m}, n \in \mathbb{Z}^+,\ \mathbf{M_{lb}} \le \mathbf{m} \le \mathbf{M_{ub}},\ 1 \le n \le N_{ub}. \end{aligned} \tag{19}$$

By inspection, for eDSA V.1 lower bound M_{lb} on m is 1, while for eDSA V.2 and V.3, the lower bound is 2. For simplicity, without loss of optimality, we take the upper bound M_{ub} on m to be λ/T. This is motivated by our intuition that, the value of m cannot exceed the average OFF duration of PU, because it would cause high collision to PU transmissions.

We also take the upper bound N_{ub} on n to be μ/T, because a higher value of n would result in low channel utilization.

For energy constrained CR nodes, e.g., in CRSNs with delay tolerant data, maximization of SU energy efficiency is of interest. This optimization problem is formulated as:

$$\begin{aligned} (P2)\ \ & \mathcal{E}_{opt}^{V_i} = \max_{\mathbf{m},n} \left\{\mathcal{E}^{V_i}(\mathbf{m}, n)\right\} \\ \text{s.t. } & R_c^{V_i}(\mathbf{m}, n) \le \eta \\ & \mathbf{m}, n \in \mathbb{Z}^+,\ \mathbf{M_{lb}} \le \mathbf{m} \le \mathbf{M_{ub}},\ 1 \le n \le N_{ub}. \end{aligned} \tag{20}$$

The optimization problems $P1$ and $P2$ are nonconvex non-linear integer programming problems, as data transmission phase lengths m, or m_1, m_2, and m_3, and spectrum sensing phase length n are integers and the objective function is nonconvex. To solve, we use branch-and-bound algorithm for nonconvex mixed-integer non-linear problems (MINLPs) [32].

In branch-and-bound algorithm, lower and upper bounds of the objective function are obtained for the sub-intervals in the domain. On the basis of feasibility and optimality criteria, some of the sub-intervals are excluded from search-space while the others are refined to narrow down the search for global optimal solution. Integer constraint on variables $\mathbf{m}$ and n in $P1$ and $P2$ are relaxed to form a non-linear problem in the continuous domain. These are further relaxed to form a convex non-linear problem ($P1_R$ and $P2_R$) in a sub-interval of interest. Relaxed convex problem is solved in the sub-intervals to obtain the lower bound. The upper bound $\mathcal{U}$ is obtained by evaluating the original problem ($P1$ or $P2$) at the optimal point obtained in lower bound computation. As $P1$ and $P2$ are evaluated at the integer points, the optimal points obtained from solving the relaxed problem are rounded off for the upper bound computation. The steps involved in the branch-and-bound algorithm are enumerated as follows:

1) Initialize search: Set $\mathcal{U} = \infty$, $\mathcal{D}$ to a single domain $\mathcal{S} \equiv \{\mathbf{m} \in [\mathbf{M_{lb}}, \mathbf{M_{ub}}],\ \ n \in [1, N_{ub}]\}$.
2) Choose a sub-interval: If $\mathcal{D} = \varnothing$, go to step 8. Else choose a sub-interval $\mathcal{S}$ from a list of regions in $\mathcal{D}$.
3) Tighten the bound: Change the lower bound on each variable in $\mathcal{S}$ to $\lceil m_{lb} \rceil$ and $\lceil n_{lb} \rceil$, and upper bound to $\lfloor m_{ub} \rfloor$ and $\lfloor n_{ub} \rfloor$.
4) Lower bound in $\mathcal{S}$: Form an integer relaxed convex problem in the domain $\mathcal{S}$ and compute the optimal point $\Omega^{\mathcal{S},l}$ of the relaxed function in $\mathcal{S}$. Go to step 7 if problem is infeasible or $\Omega^{\mathcal{S},l} > \mathcal{U}$.
5) Upper bound in $\mathcal{S}$: Using the lower bound points obtained in step 3, solve the exact problem $P1$ or $P2$ to obtain the upper bound $\Omega^{\mathcal{S},u}$ of the problem in $\mathcal{S}$. If $\Omega^{\mathcal{S},u} > \mathcal{U}$ or the problem is infeasible, go to step 6. Else set $\mathcal{U} = \Omega^{\mathcal{S},u}$. Delete all sub-intervals $\mathcal{V}$ from $\mathcal{D}$ if $\Omega^{\mathcal{V},l} > \mathcal{U}$.
6) Branching: Branching the sub-interval $\mathcal{S}$, by partitioning along the optimal value of m in $\Omega^{\mathcal{S},u}$. Include the formed sub-intervals back in $\mathcal{D}$.
7) Delete sub-interval: Delete sub-interval $\mathcal{S}$ from $\mathcal{D}$. Go to step

$$\Phi^{V_1}(\mathbf{m}, n) = \frac{\sum_{s\in\mathcal{S}}\{\pi^{V_1}(DT_s) \cdot (m\Phi_t + \Phi_s + (n-1)\Phi_i) + \pi^{V_1}(CS_s) \cdot (\Phi_s + \Phi_i \cdot (n-1))\}}{T\sum_{s\in\mathcal{S}}\{(m+n)\pi^{V_1}(DT_s) + n\pi^{V_1}(CS_s)\}}. \tag{12}$$

$$\Phi^{V_2}(\mathbf{m}, n) = \frac{\sum_{s\in\mathcal{S}}\{\pi^{V_2}(DT_s) \cdot ((m-1)\Phi_t + \Phi_s) + \pi^{V_2}(CS_s) \cdot (\Phi_s + \Phi_i \cdot (n-1))\}}{T\sum_{s\in\mathcal{S}}\{m\pi^{V_2}(DT_s) + n\pi^{V_2}(CS_s)\}}. \tag{13}$$

$$\Phi^{V_3}(\mathbf{m}, n) = \frac{\sum_{s\in\mathcal{S}}\{\sum_{j=1}^{3}((m_j-1)\Phi_t + \Phi_s)\pi^{V_3}(DT_s^j) + (\Phi_s + \Phi_i \cdot (n-1))\pi^{V_3}(CS_s)\}}{T\sum_{s\in\mathcal{S}}\{\sum_{j=1}^{3}\{m_j\pi^{V_3}(DT_s^j) + n\pi^{V_3}(CS_s)\}\}}. \tag{14}$$

2.

8) If $\mathcal{U} = \infty$, problem is infeasible. Else the optimal solution is $\mathcal{U}$.

In [33], it was shown that branch-and-bound algorithm for integer problems terminates finitely to the global minima.

We now discuss how an integer-relaxed convex problem is formulated at step 4 of the above algorithm to compute the lower bound. The numerator in $\mathcal{G}^{V_i}$ and $\mathcal{E}^{V_i}$ comprise of $p_s(l,s)$, that is computed from (8). This computation requires the sum of elements of matrix $\mathbf{Q}_s$ raised to power l (i.e., $\mathbf{Q}_s^l$). $\mathbf{Q}_s$ is an upper triangular square matrix. By employing the method in [34], we obtain a polynomial expression for each resulting element ${}_kL_{i,j}$ of the matrix L raised to power k as

$$ {}_kL_{i,j} = \sum_{r=1}^{num(i,j)} \sum_{s=1}^{mpy(r)} c_{i,j,r,s} \binom{k-1}{s-1} L_{i,j,r}^{k-s}. \quad (21) $$

The coefficients $c_{i,j,r,s}$ are computed using the sum of adjusted chains in the matrix L, as described in [34]. $num(i,j)$ is the number of unique diagonal elements between and including rows i and j, $\{L_{i,j,r}\}_{r=1}^{num(i,j)}$ is a set of these unique diagonal elements, and $mpy(r)$ is the multiplicity of $L_{i,j,r}$. Further, $p_s(l,s)$ involves summation of elements of $\mathbf{Q}_s^l(s, z/i)$ from $i = \lfloor l \cdot (1-k_e) \rfloor$ to $l-1$ which is dependent on l. To obtain this summation, the ith element of $\mathbf{Q}_s^l(s, z/i)$ is multiplied by $\delta_i(l) = 0.5\{\tanh(\beta(i - l \cdot (1-k_e)) - \tanh(\beta(i-l))\}$ (β is a constant) and all the elements are added. $\delta_i(l) \approx 1$ when i lies between $\lfloor l \cdot (1-k_e) \rfloor$ and $l-1$, and $\delta_i(l) \approx 0$ otherwise. Similar situation arises for the computation of $E_p(l,s)$ from (9) and a similar method is used for its computation.

Next we turn to the computation of steady state probabilities in the FSM representation of the protocol variants. Computation of one-step transition probability matrix $\mathbf{W}_{V_i}$ requires the computation of $\mathbf{P}^m$ and $\mathbf{P}^n$. $\mathbf{P}$ is diagonalised to obtain $\mathbf{P}^m$ and $\mathbf{P}^n$ in closed form. Steady state probabilities from $\mathbf{W}_{V_i}$ are obtained by solving the system of linear equations.

Putting these together, we obtain the closed form expressions for SU goodput, SU energy efficiency, and PU collision ratio, which are nonconvex. Objective function of the convex relaxed problem is constructed by adding a convex quadratic term [35] to the nonconvex problem, which is:

$$ (P1_R) \quad \max_{\mathbf{m},n} \left\{ \mathcal{G}^{V_i}(\mathbf{m},n) - \alpha \sum_{i \in \mathbf{m},n} (i_{lb} - i)(i_{ub} - i) \right\} $$

where $\alpha \geq \max \left\{ 0, -\frac{1}{2} \min_{\substack{i \in \mathbf{m},n \\ i_{lb} \leq i \leq i_{ub}}} \lambda^{(P1)} \right\}$, $\mathbf{m}, n \in \mathbb{R}^+$. $\lambda^{(P1)}$ is the eigen value of Hessian matrix of integer relaxed $-\mathcal{G}^{V_i}(\mathbf{m},n)$. In [35], the authors have proved that objective function formed by adding a convex quadratic term as shown above makes the resulting objective function convex in a given region of interest. Convex relaxation of $P2$ and constraint function $R_c^{V_i}(\mathbf{m},n)$ are similarly formulated.

5 On-Board Protocol Operation

5.1 Optimal packet length and back-off durations

Optimal parameters in problems $P1$ and $P2$ in (19) and (20) are computed using branch-and-bound algorithm (cf. Section 4.8). At each step of the algorithm, integer relaxed convex problem is solved to compute the lower bound, which is highly complex. The computation of probability of successful packet transmission ($p_s(l,s)$), expected number of slots with PU collision ($E_p(l,s)$), and steady state probabilities of FSM ($\underline{\pi}^{V_i}$) in closed form are highly computationally intensive and time consuming. Further, the addition of convex quadratic term in $P1_R$, which requires Hessian of the integer relaxed $\mathcal{G}^{V_i}(\mathbf{m},n)$, introduces another dimension to complexity. The worst case algorithm complexity of branch-and-bound algorithm is that of an exhaustive search.

SUs need to adjust their operating parameters ($\mathbf{m}$, n) with the changing PU traffic parameters for optimal performance. Since this is computationally intensive, online computation of optimal parameters can take significant amount of time. So, for faster adaptation of optimal packet size and inter-sensing time at different PU traffic intensities, we suggest to form a small look-up table. The table (shown in Section 6.2) consists of optimal operating parameters ($\mathbf{m}$ and n) corresponding to the different PU traffic parameters λ and μ. These optimal operating parameters are computed offline and stored in the SU memory. This look-up table is used to adapt with the changing PU traffic. In a dynamic PU traffic scenario, SU estimates the parameters λ and μ (as discussed in Section 5.3) and then consult the look-up table for the corresponding optimal $\mathbf{m}$ and n. Thus, with the help of a small database the SU is able to achieve the optimal and energy-efficient system performance.

5.2 Low-complexity pattern search algorithm

In practice, the range of λ and μ for a particular PU channel may be large. In such a case, the look-up table may be sparse and may not contain all the entries corresponding to each λ and μ. For the λ and μ values that are not present in the look-up table, we propose a low complexity algorithm which could make use of the provided look-up table and come up with the optimal operating parameters $\mathbf{m}$ and n on the fly. We use augmented Lagrange pattern search method [36] for solving the problem. The choice of this method is influenced by the following three reasons. Firstly, forming integer relaxed problem and computing gradients for the objective and the constraint is troublesome and requires high computations. Secondly, in pattern search, the objective and constraints are evaluated at discrete points, which suits well for integer constrained $\mathbf{m}$ and n. Lastly, as the number of variables involved is low, convergence is fast for this algorithm. Consider dim as the number of parameters to be computed. For eDSA V.1 and V.2 $dim = 2$, while for eDSA V.3, $dim = 4$. Algorithm 1 presents the steps involved in solving problem ($P1$) using the augmented Lagrange pattern search method. For a given Lagrange parameter $l^{(k)}$ and penalty factor $\tau^{(k)}$, augmented Lagrange function $\mathscr{L}$ in step 9 is maximized (in the inner loop) using the pattern search method. The outer loop updates the Lagrange and penalty parameters at each iteration.

Convergence properties for this algorithm have been proved in [36]. Since the algorithm starts with a better initial point provided by the look-up table, it is expected to converge fast with low computational complexity. The algorithm steps for solving ($P2$) is developed on the similar lines. The performance of the algorithm is presented in Section 6.2.

5.3 Channel parameter estimation

In practice, e.g., in cellular bands, the PU traffic is expected to change with time. Optimal performance of SU depends on the

Algorithm 1: Augmented Lagrange pattern search algorithm.

1. Convert the inequality constraint in $(P1)$ to equality constraint by using slack variable $s \geq 0$;
2. Identify the entries in the look-up table that are closest to the given λ and μ and compute the SU goodput and PU collision ratio for the corresponding $\mathbf{m}$ and n parameters for these entries at the given λ and μ;
3. Obtain a feasible parameter set (the set which satisfies $R_c \leq \eta$) that offers the highest goodput. Call this set as $\mathbf{x}_{0,0}$ (comprises of $\mathbf{m}$, n, and $s = 0$);
4. Initialize $l^{(0)}, \kappa_0, \tau_0, \omega_0, \Omega < 1, \gamma_1 < 1, \delta^* \ll 1, \kappa^* \ll 1, \alpha_\omega, \beta_\omega, \alpha_\kappa, \beta_\kappa, \xi$, and $\epsilon < 1$;
5. Set $\tau^{(0)} = \tau_0, \alpha^{(0)} = \min(\tau^{(0)}, \gamma_1), \omega^{(0)} = \omega_0(\alpha^{(0)})^{\alpha^\omega}, \delta^{(0)} = \frac{\omega^{(0)}}{1+l^{(0)}+1/\tau^{(0)}}, \kappa^{(0)} = \kappa_0(\alpha^{(0)})^{\alpha_\kappa}$, and $k = 0$;
while $k < \xi$ **do**
  6. Consider the direction vectors $D = \{e_j, -e_j\}$ $\forall\, j = 1, \cdots, dim + 1$, where e_j is a unit vector in the direction of the jth axis;
  7. Initialize $\Delta > 0$ and $j = 0$;
  while $\Delta \geq \delta^{(k)}$ **do**
    8. Compute $\chi = \eta - R_c^{V_i} - s$, and $\mathscr{L} = \mathcal{G}^{V_i} + l^{(k)}\chi - \frac{(\chi)^2}{2\tau^{(k)}}$ for each point in set $\mathbf{x}_{k,j} + \Delta D$. $\mathbf{m}$ and n are rounded to nearest integer in $m \geq 2$ and $n \geq 1$;
    9. Obtain $y = max\ \mathscr{L}$. If $y > \mathscr{L}(\mathbf{x}_{k,j})$, then $\mathbf{x}_{k,j+1} = arg\ max\ \mathscr{L}$. Else $\Delta \rightarrow \epsilon\Delta$ and set $\mathbf{x}_{k,j+1} = \mathbf{x}_{k,j}$;
    10. $j = j + 1$;
  end
  11. $\mathbf{x}_{k+1,0} = \mathbf{x}_{k,j}$ and $\Xi^{(k)} = \chi(\mathbf{x}_{k,j})$;
  if $\Xi^{(k)} \leq \kappa^{(k)}$ **then**
    if $\delta^{(k)} \leq \delta^*$ *and* $\Xi^{(k)} \leq \kappa^*$ **then**
      STOP
    end
    12. Update $l^{(k+1)} = l^{(k)} + \Xi^{(k)}/\tau^{(k)}, \tau^{(k+1)} = \tau^{(k)}, \alpha^{(k+1)} = \min(\tau^{(k+1)}, \gamma_1), \omega^{(k+1)} = \omega^{(k)}(\alpha^{(k+1)})^{\beta_\omega}, \delta^{(k+1)} = \frac{\omega^{(k+1)}}{1+l^{(k+1)}+1/\tau^{(k+1)}}$, and $\kappa^{(k+1)} = \kappa^{(k)}(\alpha^{(k+1)})^{\beta_\kappa}$;
  end
  else
    13. Update $l^{(k+1)} = l^{(k)}, \tau^{(k+1)} = \Omega\tau^{(k)}, \alpha^{(k+1)} = \min(\tau^{(k+1)}, \gamma_1), \omega^{(k+1)} = \omega_0(\alpha^{(k+1)})^{\alpha_\omega}, \delta^{(k+1)} = \frac{\omega^{(k+1)}}{1+l^{(k+1)}+1/\tau^{(k+1)}}$, and $\kappa^{(k+1)} = \kappa_0(\alpha^{(k+1)})^{\alpha_\kappa}$;
  end
  14. $k = k + 1$;
end

precise knowledge of the PU traffic parameters. For practical realizability, a channel parameter estimation algorithm is presented below for the proposed protocol variants.

SUs operation over the channel is initiated by using arbitrarily chosen low values of sensing and data transmission parameters ($\mathbf{m}$ and n). Past PU activity history could also be used to set the initial values. The SU maintains four counters: α_1, α_0, β_1, and β_0. All counters are initialized to 0. On successful data packet transmission, SU increments α_0 by the amount equal to the number of slots over which the data transmission was successful. Similarly, the SU increments the α_1 counter by the number of slots it spent in the spectrum sensing phase. The counter β_0 is incremented by 1 every time the SU transits from data transmission to spectrum sensing phase. Similarly, β_1 is incremented by 1, every time the SU transits from spectrum sensing to data transmission phase. To obtain the steady state, after the β_0 or β_1 reaches a large value (say, 100), the SU estimates the new λ_e and μ_e for the channel as $\lambda_e = \frac{\alpha_0}{\beta_0}, \mu_e = \frac{\alpha_1}{\beta_1}$. SU draws the new operating parameters $\mathbf{m}$ and n from the look-up table each time it estimates a new value of PU traffic parameters. SU repeats this process to dynamically adapt with the current traffic parameters.

TABLE 2: Default system parameters used for performance results.

Block coding ratio, k_c	0.6
Allowable error ratio, k_e	0.2
Channel bandwidth	10 Mbps
Default time slot duration, T	100 μs
Data transmission per slot, b	1 Kb
Overhead per packet, H	50 bits
Sensing energy per slot, Φ_s	4 μJ
Transmission energy per slot, Φ_t	6.95 μJ
Idle energy consumption per slot, Φ_i	1.69 μJ
PU collision ratio threshold, η	0.05
Probability of misdetection, p_{md}	0.05
Probability of false alarm, p_{fa}	0.05
Fading margin, F	10 dB
Channel frequency, f_c	2 GHz

6 Results

In this section we present the numerical and hardware system experiment assisted simulation results on the achievable SU goodput and SU energy efficiency, along with PU collision performance in the proposed eDSA variants. The system parameters used are listed in Table 2.

In general, communication systems use various forward error correcting codes ranging from convolution codes to turbo codes. The encoding rate ranges from 0.5 to 0.75 in most cases. As a case study, we take the block coding ratio $k_c = 0.6$. Error correcting capability depends on the block coding ratio and encoding technique. We take the allowable error ratio $k_e = 0.2$. SU energy consumptions are taken from [37]. From practical observations on PU activity over ISM bands, it was shown in [2] that the average idle and busy periods typically lie in the range of a few milliseconds. Hence, we consider μ and λ on the order of ms. We consider a slow fading channel where $f_D T < 0.1$ with Doppler frequency $f_D = v_c f_c / c = 50$ Hz, corresponding to SU velocity $v_c = 7.5$ m/s and fading margin F as 10 dB. Here, c is speed of light in vacuum.

6.1 Effects of operating parameters on performance

Firstly, we show the effect of m (number of slots in data transmission phase) and n (number of slots in spectrum sensing phase) on SU goodput in eDSA V.1 and eDSA V.2. We take the parameters as shown in Table 2, with average ON period of 3 ms and average OFF periods of 5 ms. For eDSA V.3, there are several parameters, namely, m_1, m_2, m_3, and n. Hence it is difficult to show the variation of metrics with respect to all these parameters. Therefore, we skip these graphs. However, eDSA V.3 is similar to eDSA V.2 and hence the necessary conclusion on eDSA V.3 can be derived by determining the behavior of eDSA V.2 of the protocol.

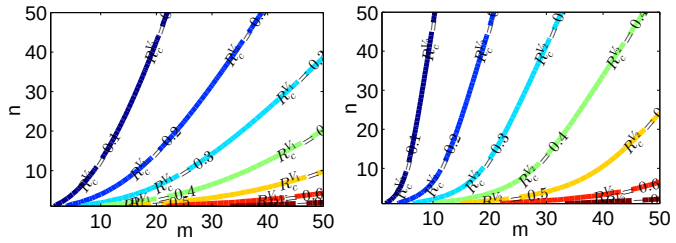

(a) eDSA V.1 (b) eDSA V.2

Fig. 7: Contour plots showing the variation of PU collision ratio with the change in m and n in eDSA V.1 and eDSA V.2, with $\lambda = 5$ ms, $\mu = 3$ ms, $f_D = 50$ Hz, and $T = 100$ μs.

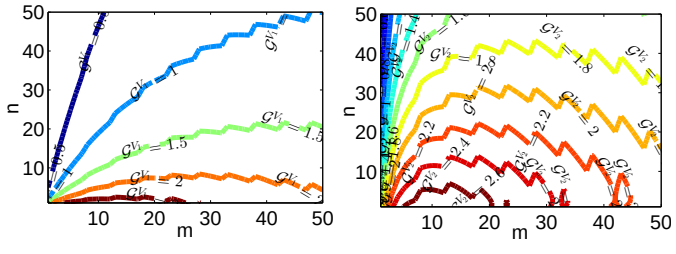

(a) eDSA V.1 (b) eDSA V.2

Fig. 8: Contour plots showing the variation of SU goodput (Mbps) with the change in m and n in eDSA V.1 and eDSA V.2, with $\lambda = 5$ ms, $\mu = 3$ ms, $f_D = 50$ Hz, and $T = 100$ μs.

Fig. 7 shows the variation in the PU collision ratio R_c with the variation in m and n for eDSA V.1 and eDSA V.2. In both cases, we observe that the PU collision increases with increase in m while it decreases with the increase in n. The reason is that, as m increases, the number of slots for the SU data transmission phase increases, and hence there are more chances of collision. Further, for a fixed m, with the increase in n most of the time SU remains in idle mode and therefore PU operation is unaffected.

The contour plots in Fig. 8 show the variation of goodput $\mathcal{G}$ with the number of slots in the data transmission phase m and spectrum sensing phase n for eDSA V.1 and eDSA V.2. From the plots it can be concluded that the goodput $\mathcal{G}$ increases with the increase in m. As the number of slots allocated for transmission is increased, it results in more opportunity to transmit. However, as the number of slots is further increased in data transmission phase, the PU collision also increases, which results in reduction of goodput. The increase of n results in decreasing goodput as SU is in idle mode in more number of slots. In computation of probability of successful packet transmission in (8), the summation is done from $\lfloor (1-k_e)l \rfloor$ to l. The rounding-off of $(1-k_e)l$ results in a saw-tooth nature in the goodput variation plots. We also observe that the goodput in eDSA V.2 is always better than the goodput in eDSA V.1 because eDSA V.2 achieves a higher channel utilization by repeated packet transmissions over the idle channel.

Fig. 9 shows the contours of energy efficiency $\mathcal{E}$ with the change in m and n. In the spectrum sensing phase, SU either senses the channel or remains idle. Hence energy consumption in this phase is less than the consumption in data transmission phase. As n increases, $\mathcal{E}$ reduces, while with increase in m $\mathcal{E}$ increases. At high values of m, goodput $\mathcal{G}$ decreases due to high collisions with PU. However, the energy consumption in this case increases resulting in lower $\mathcal{E}$.

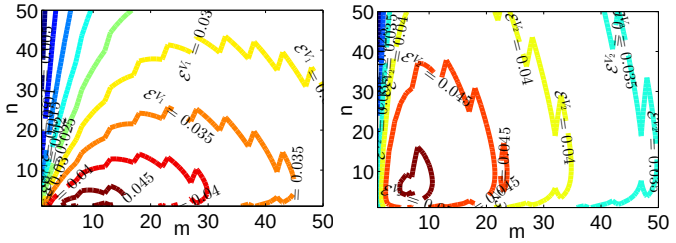

(a) eDSA V.1 (b) eDSA V.2

Fig. 9: Contour plots on SU energy efficiency (Mb/mJ) with the change in m and n in eDSA V.1 and eDSA V.2, with $\lambda = 5$ ms, $\mu = 3$ ms, $f_D = 50$ Hz, and $T = 100$ μs.

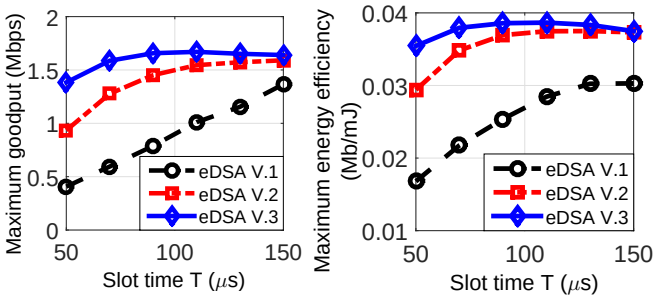

(a) Maximized $\mathcal{G}$ (b) Maximized $\mathcal{E}$

Fig. 10: SU energy efficiency versus slot time T with $\lambda = 10$ ms, $\mu = 10$ ms, $\eta = 0.05$, and $v_c = 15$ m/s.

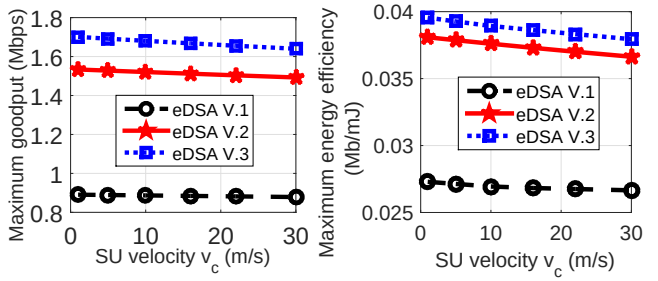

(a) Maximized $\mathcal{G}$ (b) Maximized $\mathcal{E}$

Fig. 11: $\mathcal{G}$ and $\mathcal{E}$ versus SU velocity with $\lambda = 10$ ms, $\mu = 10$ ms, $\eta = 0.05$, and $T = 100$ μs.

The optimization problems formulated in (19) and (20) for maximizing respectively, $\mathcal{G}$ and $\mathcal{E}$ under the given constraint of maximum PU collision ratio η are solved to obtain the optimized performance of the protocol in the given scenario.

Optimized performance of eDSA protocol variants versus slot size T is shown in Fig. 10. For smaller T, the sensing time (1 slot) also decreases, resulting in higher p_{fa} and p_{md} (cf. (6) and (7)). Though optimal $\mathbf{m}$ and n (in slots) also increase with the decrease in T, the total transmission time decreases so as to compensate for increased p_{md}. Hence, a lower T results in higher SU packet collisions and missed transmission opportunities, thereby reducing $\mathcal{G}$ and $\mathcal{E}$ – as seen respectively in Figs. 10a and 10b. A higher value of T results in a more accurate channel sensing, however, at the cost of high sensing time overhead. Hence, with increased T the system performance attains a maximum and eventually decreases.

Fig. 11 shows performance of the optimized eDSA variants versus SU mobility. A slight decrease in performance with the

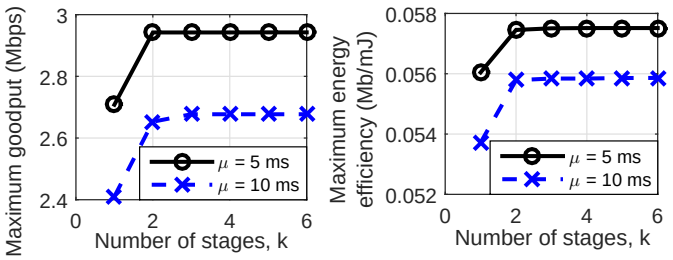

(a) Maximized $\mathcal{G}$ (b) Maximized $\mathcal{E}$

Fig. 12: Goodput and energy efficiency versus k (number of stages) in eDSA V.3 with λ = 16 ms, η = 0.05, and T = 100 μs.

increase in SU velocity is observed. Increase in SU velocity gives rise to high SU channel fading ($f_D = v_c f_c/c$). This results in high transmission loss of the SUs, which reduces the $\mathcal{G}$ and $\mathcal{E}$. The optimization problem takes into account the fading effect while computing the optimal $\mathcal{G}$ and $\mathcal{E}$. Hence the optimal parameters $\mathbf{m}$ and n are suitably adjusted to reduce the impact of channel fading on SU performance.

Before proceeding with relative performance results, we study the optimal value of k in eDSA V.3. It may be recalled, in our analysis we have considered $k = 3$. To study the effect of k on SU performance, Fig. 12 plots the SU goodput and energy efficiency with k ranging from 1 to 6. It is observed that the performance of SU initially increases with increase in k, and then saturates beyond $k \geq 3$. This observation suggests that the optimal value of k can be safely considered 3, as further increase in k can be detrimental in terms of cost of computation (for determining optimal parameters and on variable packet fragmentation) without offering any additional SU performance benefits. Relative performance of the competitive protocols is discussed next.

6.2 Protocol performance comparison

The performances of eDSA protocol variants are compared with VX DSA [7] and RIBS [8] that have the closest system settings. In VX DSA, if the SU senses the channel as idle, it transmits a packet of length l_s and subsequently goes to vacation (idles) for duration v_s. If the channel is sensed busy, SU vacates for $l_s + v_s$ duration. SU senses the channel again after vacation, and the process repeats. Optimal SU packet length l_s for maximizing its goodput is obtained and the corresponding SU energy efficiency is computed. For maximizing goodput, vacation period v_s was considered 0. The authors did not deal with energy efficiency optimization (i.e., optimum v_s) aspect of the protocol. The performance of the other protocol variants in [7] are close to that of VX DSA.

In RIBS, the SU generates a channel sensing schedule based on exponentially distributed random back-off. SU waits for the scheduled back-off time and senses the channel. If the channel is sensed idle, SU transmits frames up to duration y_{max} and again senses the channel following the sensing schedule. We obtain via simulations the optimal SU packet length y_{max} in RIBS that meets the PU collision constraints. Similarly as in [8], simulations are performed for three different exponential back-off (BO) counter values with their respective mean values ($\mathbb{E}[BO]$) equal to $0.1y_{max}$, y_{max}, and $5y_{max}$.

We consider various scenarios with different PU activity. μ is fixed to 5 ms while λ is varied from 2 ms to 16 ms. The PU collision ratio threshold is set to $\eta = 0.05$. For each PU activity

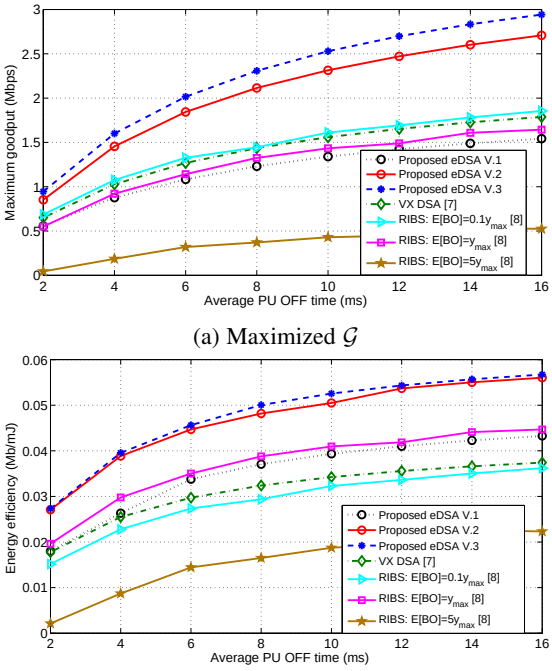

(a) Maximized $\mathcal{G}$

(b) Corresponding $\mathcal{E}$

Fig. 13: Optimized goodput performance versus PU traffic intensity with $T = 100$ μs, $\mu = 5$ ms, $\eta = 0.05$, and $f_D = 50$ Hz.

TABLE 3: Optimum protocol parameters for maximized goodput under different PU traffic conditions with slot size $T = 100$ μs, $\mu = 5$ ms, $\eta = 0.05$, and $f_D = 50$ Hz.

PU average OFF (ms)	eDSA V.1		eDSA V.2		eDSA V.3			
	m	n	m	n	m_1	m_2	m_3	n
2	2	3	4	7	2	5	5	4
4	2	3	4	7	2	4	5	4
6	4	6	4	7	2	3	5	4
8	4	6	4	7	2	5	5	5
10	4	6	4	7	2	5	5	5
12	4	6	5	13	2	5	5	5
14	4	6	5	13	2	5	5	5
16	4	6	5	13	2	5	5	5

case, we obtain the optimal system parameter values, i.e., SU packet lengths (m or m_1, m_2, m_3) and SU inter-sensing times (n), for the eDSA protocol variants by solving the two optimization problems. Maximum goodput and energy efficiency achieved by the SUs operating with the proposed protocols are compared with the metrics obtained in VX DSA scheme and RIBS.

Fig. 13 shows the maximized goodput and corresponding energy efficiency with the variation in primary traffic parameters. We observe that the eDSA V.1 protocol has a lower goodput than eDSA V.2. However goodput of eDSA V.3 is best. eDSA V.1 performs poorly as it does not fully exploit the idle times in the spectrum. eDSA V.3 performs better than eDSA V.2 because of the variation of the SU packet lengths in successive data transmission phases, which helps reduce the PU collision probability and increase SU goodput. The corresponding energy efficiency of eDSA V.3 is slightly higher than eDSA V.1 and eDSA V.2. This is because eDSA V.3 provides a high throughput with the similar sensing overheads, as the SU packets of larger size are transmitted. Table 3 presents the optimal system parameter values for different PU traffic parameters for this optimization problem.

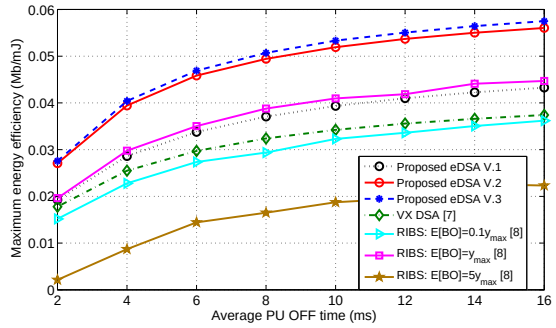

(a) Maximized $\mathcal{E}$

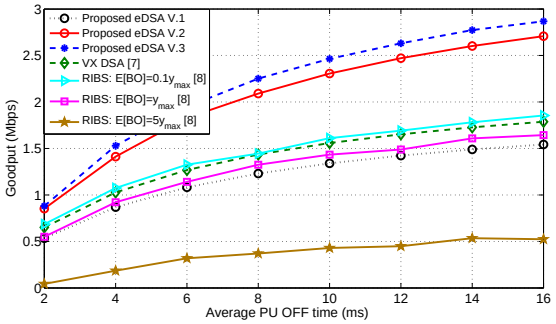

(b) Corresponding $\mathcal{G}$

Fig. 14: Optimized energy efficiency performance versus PU traffic intensity with $T = 100$ μs, $\mu = 5$ ms, $\eta = 0.05$, and $f_D = 50$ Hz.

TABLE 4: Optimal protocol parameters for maximized energy efficiency under different PU traffic conditions with $T = 100$ μs, $\mu = 5$ ms, $\eta = 0.05$, and $f_D = 50$ Hz.

PU average OFF (ms)	eDSA V.1		eDSA V.2		eDSA V.3			
	m	n	m	n	m_1	m_2	m_3	n
2	4	6	4	7	3	6	5	7
4	4	6	5	12	2	5	6	8
6	4	6	5	12	2	5	6	9
8	4	6	5	13	2	4	6	9
10	4	6	5	13	2	5	6	10
12	4	6	5	13	2	4	6	10
14	4	6	5	13	2	4	6	10
16	4	6	5	13	2	5	6	11

The proposed eDSA V.2 and eDSA V.3 outperform VX DSA and RIBS access strategies because eDSA V.2 and V.3 utilize most of the vacant spaces in the spectrum. In VX DSA, SU goes into vacation for duration l_s whenever the channel is found busy, which adds to the channel's idle phase discovery delay. Random back-off after each channel access instance in RIBS reduces the channel utilization, and hence lowers the SU goodput. RIBS scheme with $\mathbb{E}[BO] = 0.1y_{max}$ has a higher goodput than with other $\mathbb{E}[BO]$ values because with $\mathbb{E}[BO] = 0.1y_{max}$, channel is accessed more frequently, resulting in a higher idle channel utilization. However, due to more frequent channel sensing in $\mathbb{E}[BO] = 0.1y_{max}$, its energy efficiency is low.

Fig. 14 shows maximized energy efficiency and the corresponding goodput in the eDSA variants, VX DSA, and RIBS. Here as well, eDSA V.3 outperforms the other versions. eDSA V.3 allows the value of n to be large while keeping the goodput maintained at a reasonably high value. The corresponding goodput plot shows that, in-spite of n being large in eDSA V.3, the goodput remains comparable to eDSA V.2, while it is mostly higher than

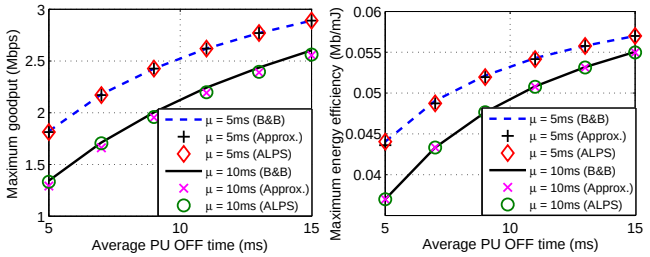

(a) Maximized $\mathcal{G}$ (b) Maximized $\mathcal{E}$

Fig. 15: Optimized goodput and energy efficiency performance of eDSA V.3 versus PU traffic intensity with different parameter estimation options. $T = 100$ μs, $f_D = 50$ Hz, and $\eta = 0.05$. (B&B: branch-and-bound algorithm; Approx.: look-up table approximation; ALPS: augmented Lagrange pattern search algorithm)

eDSA V.1, because of optimally varied packet size in successive transmissions in eDSA V.3. VX DSA and RIBS do not optimize the inter-sensing time during the channel busy period. Hence, SUs energy efficiency with VX DSA and RIBS schemes are poorer. Optimal system parameter values at different PU traffic parameters are presented in Table 4 for the maximization of $\mathcal{E}$.

As discussed in Sections 5.1 and 5.2, a look-up table is maintained by the SU which could be sparse (e.g., in a step of 2 ms in Tables 3 and 4). For obtaining the optimal $\mathbf{m}$ and n parameters for traffic parameters (λ and μ) other than the listed values in the look-up table, there are three options. One can use branch-and-bound algorithm, but it is computationally intensive. Second option is to consider the closest entry in the look-up table for the given traffic parameters and use those optimal parameters (we call it *look-up table approximation*). The third option is to use the proposed augmented Lagrange pattern search algorithm (cf. Section 5.2). Fig. 15 presents the SU performance using these three options for eDSA V.3. Look-up table comprises of four entries corresponding to $\lambda = \{5, 15\}$ ms and $\mu = \{5, 15\}$ ms. Performances of the three alternatives are observed to be closely following one another. For $\mu = 5$ ms, all the methods converge, while for $\mu = 10$ ms, there is some divergence seen in maximized goodput performance. In this case, the proposed augmented Lagrange pattern search algorithm performs marginally better than the look-up table approximation scheme. While obtaining the optimal parameters on Matlab R2014a running on Intel i7-3770 CPU with 3.4 GHz clock and 16 GB RAM, on an average, augmented Lagrange pattern search algorithm took around 0.4 sec as opposed to 16 sec in branch-and-bound algorithm. From these observations we infer that, while with a dense look-up table based approach the SU operating parameters can be readily obtained without significant performance degradation, a sparse look-up table along with augmented Lagrange pattern search algorithm can also guarantee online optimal SU performance at a reduced memory as well as computation cost.

6.3 Empirical data assisted performance studies

We now demonstrate adaptability of the proposed protocols and the associated SU performance by generating real PU traffic traces over the cellular band and ISM (2.4 GHz) band. GSM-1800 band is considered with center frequency of 1810.2 MHz and bandwidth of 200 kHz. We have used Amitec SDR kit (www.amitec.co) and obtained energy detection based channel sensing samples at 10 kHz over a period of 15 sec during daytime on a weekday. Fig. 16a

shows the actual and estimated traffic parameters. The mean PU ON period is seen to be around 5 slots which corresponds to the 0.5 ms GSM time slot. The traffic parameter estimation algorithm proposed in Section 5.3 is implemented to track the changing PU traffic parameters. Fig. 16a shows closeness of the estimated and actual traffic parameters, which proves correctness of the proposed channel estimation algorithm.

To further observe the performance of the proposed traffic estimation algorithm in a dynamic PU activity scenario, we have carried out Skype video (video over IP) call over the IEEE 802.11b WiFi network using channel 1 (center frequency 2.412 GHz, bandwidth 22 MHz). The wireless device (laptop) was connected to the WiFi router to establish a Skype call. There was no other device in the vicinity. Fig. 16b shows the actual and estimated traffic parameters. The first 5 seconds corresponds to setting up of the Skype call and the rest 10 seconds corresponds to the in-progress call. We observe that the PU channel is highly busy when the call is under progress. In this case as well, plot shows closeness of the estimated and actual traffic parameters and thus proves correctness of the proposed channel estimation algorithm.

Next, we present the empirical data assisted simulation results on the SU performance, where the PU channel occupancy measurements from GSM-1800 and Skype call experiment are used. The proposed eDSA versions are compared with VX DSA and RIBS. Channel parameter estimation algorithm is enabled in all the schemes. SU channel fading effects are not considered. Figs. 17a and 17b present the maximized goodput and energy efficiency respectively over the GSM-1800 band, while Figs. 17c and 17d present the maximized goodput and energy efficiency respectively over the ISM band. Results show that, while eDSA V.2 and V.3 are better than VX DSA and RIBS, eDSA V.3 – which optimally adjusts the packet length during consecutive data transmission phases – has the overall superior performance in terms of goodput as well as energy efficiency. Thus, the combined optimization of data packet length and inter-sensing interval is noted to be a promising approach for SU operation over a single PU channel.

6.4 Discussion

In eDSA V.1, after every packet transmission the SU remains idle for n slots to allow PUs to carry out their own transmissions. However, as the relative performance results also demonstrate, it does not make most use of the channel because, at some idling phases the PU channel may also be idle – resulting in lost transmission opportunity. To overcome this drawback, in eDSA V.2 and V.3 SU successively transmits by sensing the channel after every packet transmission. This helps the SUs make most use of the available channels. Although eDSA V.3 performs better than V.2, it requires higher computations for obtaining optimal packet lengths and inter sensing times, and it has a higher complexity in packet fragmentation into different sizes. Thus a performance-complexity tradeoff exists between eDSA V.2 and V.3.

7 Conclusion

In this paper we have proposed three protocol variants of eDSA for the SUs. The proposed approach accounts for realistic traffic and primary transmission characteristics, and the protocols are aimed at maximizing the SU channel utilization without degrading the PU performance below a predefined threshold. Via rigorous Markov modeling, SU goodput, energy efficiency, as well as PU collision ratio have been captured. Optimum data transmission and sensing parameters have been derived via two optimization formulations for maximizing respectively SU goodput and energy efficiency, and the optimization problems have been solved using branch-and-bound algorithm. To avoid time-consuming optimization, a look-up table based approach coupled with augmented Lagrange pattern search algorithm is proposed, which can be easily implemented on simple hardware. A simple PU channel activity parameter estimation technique has also been presented to dynamically adjust the SU operating parameters according to the PU traffic. The SU protocol performance have been studied by generating PU activity traces from real-time video call experiment and cellular band measurements. Results confirm that the protocol performs significantly better than the competitive DSA protocols. The proposed protocols and implementation techniques would be of interest for low-cost and energy constrained CRNs. Similar protocols can be developed for cognitive relay networks [38].

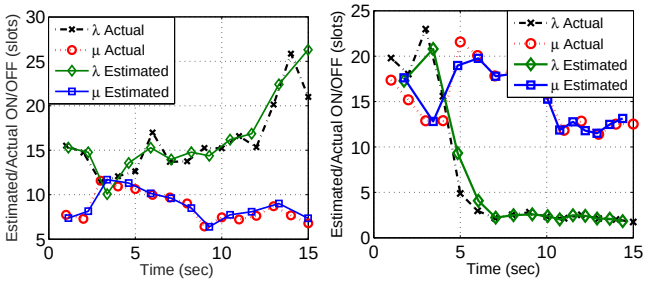

(a) Cellular band (b) ISM band

Fig. 16: PU traffic parameter estimated by SU at different time instances. Channel occupancy sample time (T) is 100 μs.

Acknowledgments

This work has been supported in parts by the ITRA Media Lab Asia project under Grant no. ITRA/15(63)/Mobile/MBSSCRN/01 and the Department of Science and Technology under Grant no. SB/S3/EECE/0248/2014.

References

[1] W. Webb, "On using white space spectrum," *IEEE Commun. Mag.*, vol. 50, no. 8, pp. 145–151, Aug. 2012.

[2] S. Geirhofer, L. Tong, and B. Sadler, "Cognitive radios for dynamic spectrum access - Dynamic spectrum access in the time domain: Modeling and exploiting white space," *IEEE Commun. Mag.*, vol. 45, no. 5, pp. 66–72, May 2007.

[3] C. Sum, G. Villardi, M. Rahman, T. Baykas, H. Tran, Z. Lan, C. Sun, Y. Alemseged, J. Wang, C. Song, C. Pyo, S. Filin, and H. Harada, "Cognitive communication in TV white spaces: An overview of regulations, standards, and technology," *IEEE Commun. Mag.*, vol. 51, no. 7, pp. 138–145, Jul. 2013.

[4] D. Willkomm, S. Machiraju, J. Bolot, and A. Wolisz, "Primary user behavior in cellular networks and implications for dynamic spectrum access," *IEEE Commun. Mag.*, vol. 47, no. 3, pp. 88–95, Mar. 2009.

[5] Y. Pei, Y.-C. Liang, K. Teh, and K. H. Li, "Energy-efficient design of sequential channel sensing in cognitive radio networks: Optimal sensing strategy, power allocation, and sensing order," *IEEE J. Sel. Areas Commun.*, vol. 29, no. 8, pp. 1648–1659, Sep. 2011.

[6] S. Huang, X. Liu, and Z. Ding, "Optimal transmission strategies for dynamic spectrum access in cognitive radio networks," *IEEE Trans. Mobile Comput.*, vol. 8, no. 12, pp. 1636–1648, Dec. 2009.

[7] ——, "Opportunistic spectrum access in cognitive radio networks," in *Proc. IEEE INFOCOM*, Phoenix, AZ, USA, Apr. 2008, pp. 2101–2109.

[8] M. Sharma and A. Sahoo, "Stochastic model based opportunistic channel access in dynamic spectrum access networks," *IEEE Trans. Mobile Comput.*, vol. 13, no. 7, pp. 1625–1639, Jul. 2014.

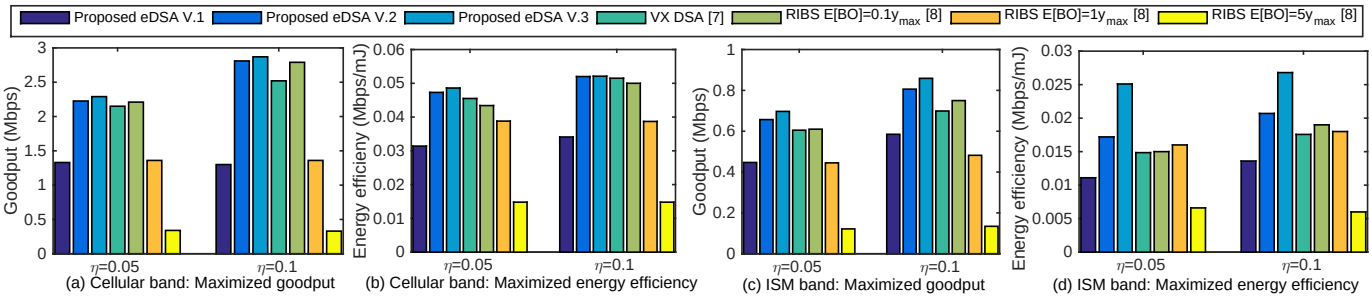

Fig. 17: Goodput and energy efficiency versus PU collision constraint η for cellular and ISM band, with $T = 100$ μs.

[9] S. Agarwal and S. De, "Impact of channel switching in energy constrained cognitive radio networks," *IEEE Commun. Lett.*, vol. 19, no. 6, pp. 977–980, Jun. 2015.

[10] S. Althunibat, M. Di Renzo, and F. Granelli, "Cooperative spectrum sensing for cognitive radio networks under limited time constraints," *Computer Commun.*, vol. 43, pp. 55 – 63, 2014.

[11] ——, "Towards energy-efficient cooperative spectrum sensing for cognitive radio networks: an overview," *Telecommun. Sys.*, vol. 59, no. 1, pp. 77–91, 2015.

[12] A. De Domenico, E. Strinati, and M. Di Benedetto, "A survey on MAC strategies for cognitive radio networks," *IEEE Commun. Survey Tuts.*, vol. 14, no. 1, pp. 21–44, Feb. 2012.

[13] H. Kim and K. Shin, "Efficient discovery of spectrum opportunities with MAC-layer sensing in cognitive radio networks," *IEEE Trans. Mobile Comput.*, vol. 7, no. 5, pp. 533–545, May 2008.

[14] K. W. Choi and E. Hossain, "Opportunistic access to spectrum holes between packet bursts: A learning-based approach," *IEEE Trans. Wirelss Commun.*, vol. 10, no. 8, pp. 2497–2509, Aug. 2011.

[15] J. Park and M. van der Schaar, "Cognitive MAC protocols using memory for distributed spectrum sharing under limited spectrum sensing," *IEEE Trans. Commun.*, vol. 59, no. 9, pp. 2627–2637, Sep. 2011.

[16] Y. Cao, D. Qu, and T. Jiang, "Throughput maximization in cognitive radio system with transmission probability scheduling and traffic pattern prediction," *Mob. Netw. Appls.*, vol. 17, no. 5, pp. 604–617, Oct. 2012.

[17] W. Zhang, C. K. Yeo, and Y. Li, "A MAC sensing protocol design for data transmission with more protection to primary users," *IEEE Trans. Mobile Comput.*, vol. 12, no. 4, pp. 621–632, Apr. 2013.

[18] Q. Chen, W. Wong, M. Motani, and Y.-C. Liang, "MAC protocol design and performance analysis for random access cognitive radio networks," *IEEE J. Sel. Areas Commun.*, vol. 31, no. 11, pp. 2289–2300, Nov. 2013.

[19] S. Jha, U. Phuyal, M. Rashid, and V. Bhargava, "Design of OMC-MAC: An opportunistic multi-channel MAC with QoS provisioning for distributed cognitive radio networks," *IEEE Trans. Wireless Commun.*, vol. 10, no. 10, pp. 3414–3425, Nov. 2011.

[20] S. Kwon, B. Kim, and B. hee Roh, "Preemptive opportunistic MAC protocol in distributed cognitive radio networks," *IEEE Commun. Lett.*, vol. 18, no. 7, pp. 1155–1158, Jul. 2014.

[21] H. Su and X. Zhang, "Opportunistic energy-aware channel sensing schemes for dynamic spectrum access networks," in *Proc. IEEE GLOBECOM*, Miami, FL, USA, Dec. 2010.

[22] R. Deng, S. He, J. Chen, J. Jia, W. Zhuang, and Y. Sun, "Energy-efficient spectrum sensing by optimal periodic scheduling in cognitive radio networks," *IET Commun.*, vol. 6, no. 6, pp. 676–684, Apr. 2012.

[23] Y. Wu and D. Tsang, "Energy-efficient spectrum sensing and transmission for cognitive radio system," *IEEE Commun. Lett.*, vol. 15, no. 5, pp. 545–547, May 2011.

[24] Z. Shi, K. Teh, and K. Li, "Energy-efficient joint design of sensing and transmission durations for protection of primary user in cognitive radio systems," *IEEE Commun. Lett.*, vol. 17, no. 3, pp. 565–568, Mar. 2013.

[25] Y. Wu, V. Lau, D. Tsang, and L. P. Qian, "Energy-efficient delay-constrained transmission and sensing for cognitive radio systems," *IEEE Trans. Veh. Technol.*, vol. 61, no. 7, pp. 3100–3113, Sep. 2012.

[26] M. Oto and O. Akan, "Energy-efficient packet size optimization for cognitive radio sensor networks," *IEEE Trans. Wireless Commun.*, vol. 11, no. 4, pp. 1544–1553, Apr. 2012.

[27] S. Wang, Y. Wang, J. Coon, and A. Doufexi, "Energy-efficient spectrum sensing and access for cognitive radio networks," *IEEE Trans. Veh. Technol.*, vol. 61, no. 2, pp. 906–912, Feb. 2012.

[28] C. Xiong, L. Lu, and G. Li, "Energy-efficient spectrum access in cognitive radios," *IEEE J. Sel. Areas Commun.*, vol. 32, no. 3, pp. 550–562, Mar. 2014.

[29] G. Shah and O. Akan, "Cognitive adaptive medium access control in cognitive radio sensor networks," *IEEE Trans. Veh. Technol.*, vol. 64, no. 2, pp. 757–767, Feb. 2015.

[30] M. Zorzi, R. Rao, and L. Milstein, "On the accuracy of a first-order Markov model for data transmission on fading channels," in *Proc. IEEE International Conference on Universal Personal Communications*, Tokyo, Japan, Nov. 1995, pp. 211–215.

[31] Y.-C. Liang, Y. Zeng, E. Peh, and A. T. Hoang, "Sensing-throughput tradeoff for cognitive radio networks," *IEEE Trans. Wireless Commun.*, vol. 7, no. 4, pp. 1326–1337, Apr. 2008.

[32] E. Smith and C. Pantelides, "Global optimization of non-convex MINLPs," *Comp. Chem. Eng.*, vol. 21, pp. S791–S796, 1997.

[33] R. Horst and H. Tuy, *Global Optimization: Deterministic approach*, 2nd ed. Berlin: Springer-Verlag, 1993.

[34] W. Shur, "A generalized close form for triangular matrix powers," May 2014, pp. 1–11. [Online]. Available: arXiv:1301.6820v2 [math.CO]

[35] C. Maranas and C. Floudas, "Global minimum potential energy conformations of small molecules," *J. Global Optimizations*, vol. 4, pp. 135–170, 1994.

[36] R. M. Lewis and V. Torczon, "A globally convergent augmented Lagrangian pattern search algorithm for optimization with general constraints and simple bounds," *SIAM J. Optim.*, vol. 12, no. 4, pp. 1075–1089, 2002.

[37] S. Maleki, A. Pandharipande, and G. Leus, "Energy-efficient distributed spectrum sensing for cognitive sensor networks," *IEEE Sensors J.*, vol. 11, no. 3, pp. 565–573, Jan. 2011.

[38] H. Huang, Z. Li, J. Si, and R. Gao, "Outage analysis of underlay cognitive multiple relays networks with a direct link," *IEEE Commun. Lett.*, vol. 17, no. 8, pp. 1600–1603, Aug. 2013.

Satyam Agarwal (S'13) received his B.Tech. in Electronics and Communication from Thapar University, India, in 2010 and M.Tech. in Electrical Engineering from IIT Kanpur in 2012. He is currently working towards the Ph.D. degree with the Department of Electrical Engineering at IIT Delhi. His research interests include cooperative communications and link layer protocol designs in wireless networks. He is a student member of IEEE and IEEE Communications Society.

Swades De (S'02-M'04-SM'14) received the Ph.D. degree from the State University of New York at Buffalo, NY, USA, in 2004. He is currently an Associate Professor in the Department of Electrical Engineering, IIT Delhi, India. In 2004, he worked as an ERCIM researcher at ISTI-CNR, Italy. From 2004 to 2006 he was with NJIT as an Assistant Professor. His research interests include performance study, resource efficiency in wireless networks, broadband wireless access, and optical communication systems.